CHARACTERISTIC CAVITATION CURVE TYPES OF HYDRAULIC TURBINES

By

Á. Fáy

Department of Hydraulic Machines, Polytechnical University, Budapest
(Received October 13, 1967)

Presented by Prof. Dr. J. Varga

Introduction

In course of cavitation tests on model hydraulic turbines, the characteristic curves can be determined by means of several different methods. Generally the $\eta-\sigma$, $P-\sigma$, $Q-\sigma$ curves pertaining to a given cavitation-free operating condition of the turbine are plotted while the turbine *head* and *speed* are maintained at constant values during the tests. Due to its obvious advantages, implicitely the same method was recommended by the draft of International Test Code for Cavitation Acceptance Tests [1]. In course of cavitation tests performed for research or design purposes, however, other methods permitting the variation of head and speed, and leading in certain cases to much more rapid measurements or advantageous from other aspects are also being made use of. The following paragraphs describe some of these techniques, and compare the characteristic curves obtained by four different methods, on the basis of tests made on one of the Kaplan model turbines of the Ganz-MÁVAG Works, with the intention of contributing to the development of such aspects whereby, in case of a given test objective, the possibly most suitable testing method could be selected.

Symbols

- Q Volumetric flow, m^3/s
- n Speed, 1/min
- M Torque, mkp (in arbitrary units for the Figures)
- H Net head of the turbine, m
- P Power output of the turbine, kW
- η Turbine efficiency
- σ Thoma cavitation number

Characteristic curve types

In course of the cavitation tests of a model turbine, in addition to the setting of guide vanes and, in case of adjustable runner blades to that of the latter, for each test point any *three* of the five main variables Q, H, n, M, σ

may be adjusted optionally within, of course, the limitations of the turbine and the test rig. The values of the other two variables are then governed by the flow itself.

In characteristic cavitation curve determinations generally a set of points is recorded by varying gradually σ. Thus, for a given σ value, *two* other variable values of the total of five referred to above may be selected optionally at each test points. Depending on how the values of these two variables are selected when measuring the set of points of the characteristic curve, different characteristic curve types may be defined.

Here only four principal types will be explained.

Test point series adjustment method		Fundamental characteristic curves measured	Symbol of the characteristic curve type
$H = \text{const},$	$n = \text{const}$	$M-\sigma$, $Q-\sigma$	A
$H = \text{const},$	$M = \text{const}$	$Q-\sigma$, $n-\sigma$	B
$H = \text{const},$	$Q/n = \text{const}$	$M-\sigma$, $Q-\sigma$, or $n-\sigma$	C
$H = \text{const},$	$M/n^2 = \text{const}$	$Q-\sigma$, $M-\sigma$, or $n-\sigma$	D

The characteristic curve point measured at a maximum σ value corresponds, generally, to the cavitation-free operating condition. The values set and measured, respectively, pertaining to the maximum σ value are called the "initial" values of the characteristic curve. These are indicated by the following symbols:

$$Q_0, \; H_0, \; n_0, \; M_0$$

When measuring any characteristic curve point, the values of the optionally adjustable *two* variables are unequivocally determined by the initial values and the *two* equations given for the type concerned.

The two equations governing characteristic curve type may obviously be given in several ways and, consequently, there are several corresponding types. Investigations on the four types in question are justified by practical reasons.

Type — A — In prototype turbine operation the variables H and n are given. Thus, from the characteristic curves $M-\sigma$ and $Q-\sigma$ of Type A, as well as from $P-\sigma$ and $\eta-\sigma$ derived therefrom, the designer can directly evaluate the effect of suction head variations. This may be the reason why Type A is the most widely accepted solution.

Type — B — The use of Type B characteristic curves may be justified by two practical reasons. Partly the torque can be maintained at a constant value by the application of simple, widely used regulators, and partly this is where the output breakdown is the steepest as demonstrated later on whereby, in turn, the "standard σ" determination [1] is most accurate in this case.

Type — C — The application of condition C ensures a constant ratio between average speed components at runner inlet. This is never accomplished with the other characteristic curve types ! Maintenance of speed ratio may be advantageous from various hydraulic considerations. If, for example, a propeller blade turbine is tested for cavitation, and the characteristic curves of a geometrically similar and in plane developed blade lattice measured in a cavitation tunnel are available, then no other but this type will prove suitable for the comparison of the records. Type C will be further characterized in the next paragraph.

Type — D — If turbine braking is done by a water brake such as the Schenck type, and the brake adjustment is kept unchanged, then the characteristic curve of the brake follows more or less the $M/n^2 = \text{const}$ rule. Thus the D-type characteristic cavitation curve conforms to the tests performed with an unchanged brake setting.

Had been the characteristic cavitation curves of the turbine measured with the *same test head* then, for any type of characteristic curve, the other types could be plotted therefrom, in the manner described in paragraph next but one, provided of course that a sufficient number of recorded characteristic curves was available.

Conversion in case of varying test head

When tests are performed with varying test heads, the characteristic curves are generally converted to the same head, by means of the usual rules:

$$\frac{n''}{n'} = \left(\frac{H''}{H'}\right)^{1/2}, \quad \frac{Q''}{Q'} = \left(\frac{H''}{H'}\right)^{1/2}, \quad \frac{M''}{M'} = \frac{H''}{H'}.$$

This process means the neglection of the scale effects due to head variations, of the Froude and Reynolds number effect, etc. Great (about ninefold) head variations actually affect cavitation [3] and, therefore, the views on the application of the laws of conversion do not agree [4], [5]. In case of minor head variations, however, there is no doubt about their validity (except in case of extremely low head turbines) [5, 6]. This opinion is reflected by the draft test code referred to earlier [1].

The neglection of scale effects due to head variations, that is, the acceptance of the conversion rules has important consequences with respect the cavitation characteristic curves. Namely, replacing variables n, Q, M by variables

$$n_{11}, \; Q_{11}, \; M_{11}$$

converted to the $H = 1m$ and $D = 1m$ values, it follows from the above equations that the characteristic curves of the same type

$$n_{11} - \sigma, \ Q_{11} - \sigma, \ M_{11} - \sigma, \ \eta - \sigma$$

recorded with different head values will coincide. This finding is supported by test results. As an example, the B-type n_{11}-curves of a Kaplan model turbine, obtained with different head values are presented (Fig. 1).

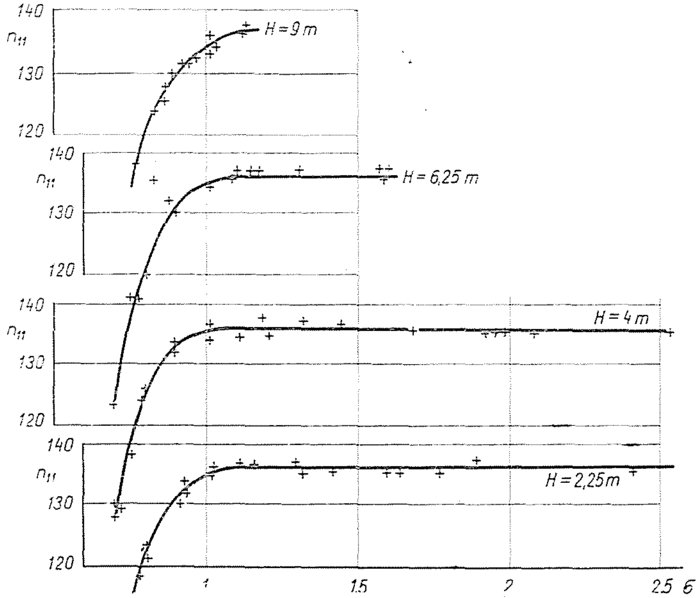

Fig. 1

Assuming the conversion laws to be valid, the number of equations characterizing the curve types can be reduced by one. It is easy to realize that the types in question satisfy the following equations:

$$A\colon n_{11} = \text{const}, \ B\colon M_{11} = \text{const}, \ C : \frac{Q_{11}}{n_{11}} = \text{const}, \ \ D : \frac{M_{11}}{{n_{11}}^2} = \text{const}.$$

If other than the four types of characteristic cavitation curves described above are also studied, and some of these curves are found to satisfy any of these equations, then it follows from the conversion formulae that the

$$n_{11} - \sigma, \ Q_{11} - \sigma, \ M_{11} - \sigma, \ \eta - \sigma$$

curves of the two types agree. Such types are considered as "equivalent".

Let us examine, for example, the characteristic curve type obtained with the head varied during test, and the test values are set to satisfy conditions

$$Q = \text{const}, \quad n = \text{const}.$$

This type has the equation $Q_{11}/n_{11} = \text{const}$ satisfied and, therefore, is equivalent to type C defined by $H = \text{const}$ and $Q/n = \text{const}$.

When recording characteristic curves type C, setting the test values is much simpler by this latter method than with the original one. The conditions $Q = \text{const}$ and $n = \text{const}$ are frequently applied for the cavitation tests of pumps, advantageous also for the development of uniform procedures.

Comparison of characteristic curves on the basis of tests

The tests were performed in the Hydraulic Machine Laboratory of the Ganz-MÁVAG Works, using a Kaplan model turbine of 200 mm runner diameter mounted into a closed turbine test rig. Test results obtained with a

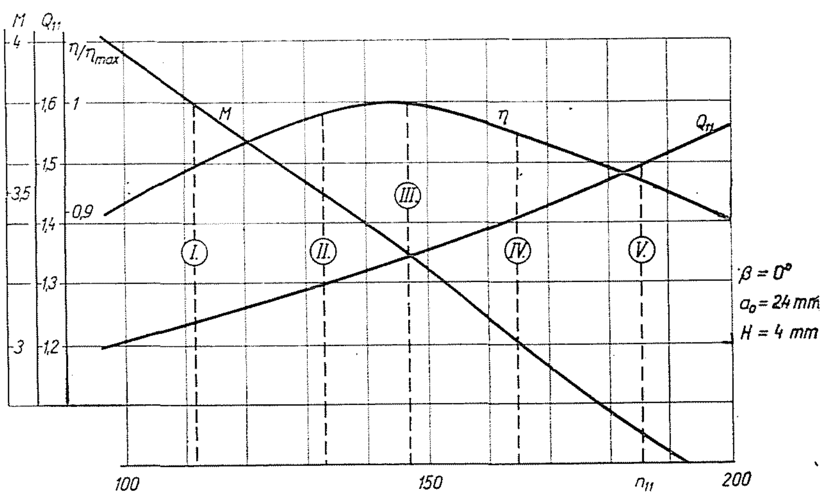

Fig. 2

single guide vane opening and a single runner blade setting are described, considered, however, to be typical.

The characteristic curves corresponding to the cavitation-free operating condition are illustrated by Fig. 2. Curves Type B have been recorded whereby Figs 3, 4 and 5 could be plotted to illustrate the displacement of the characteristic curves due to cavitation, shown in Fig. 2.

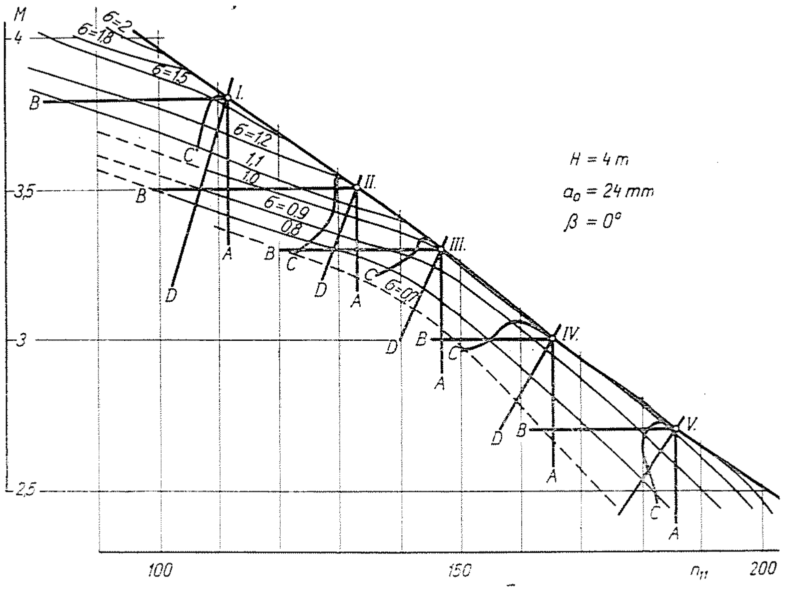
M
4
3,5
3
2,5
σ=2
σ=1,8
σ=1,5
σ=1,2
1,1
1,0
σ=0,9
0,8
σ=0,7
I.
II.
III.
IV.
V.
H = 4 m
a_0 = 24 mm
β = 0°
100
150
200
n_{11}

Fig. 3

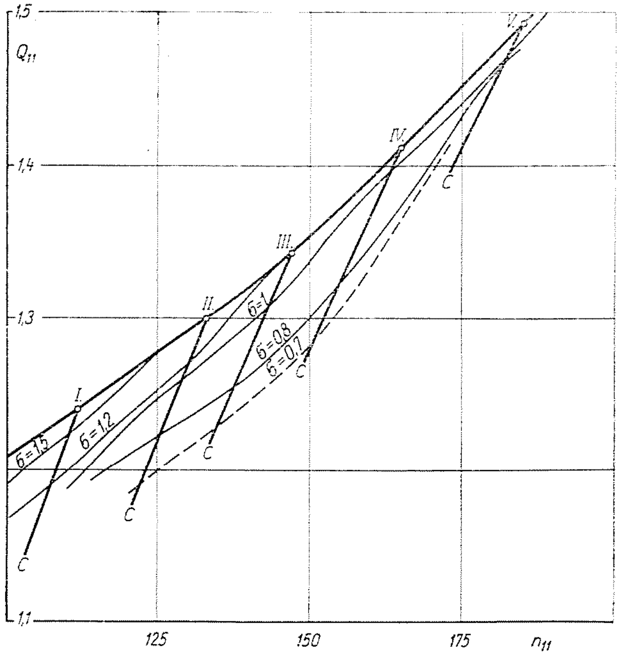
1,5
Q_{11}
1,4
1,3
1,1
I.
II.
III.
IV.
V.
σ=1,5
σ=1,2
σ=1
σ=0,8
σ=0,7
125
150
175
n_{11}

Fig. 4

The head was of the same value in course of the tests.

Along the characteristic curves representing the cavitation-free operating conditions, each point as an initial value has an A, B, C, and D type curve associated with. Five such points (marked I to V) were selected (Fig. 2) and the A, B, C, D type characteristic curves were plotted for each, in the manner described below.

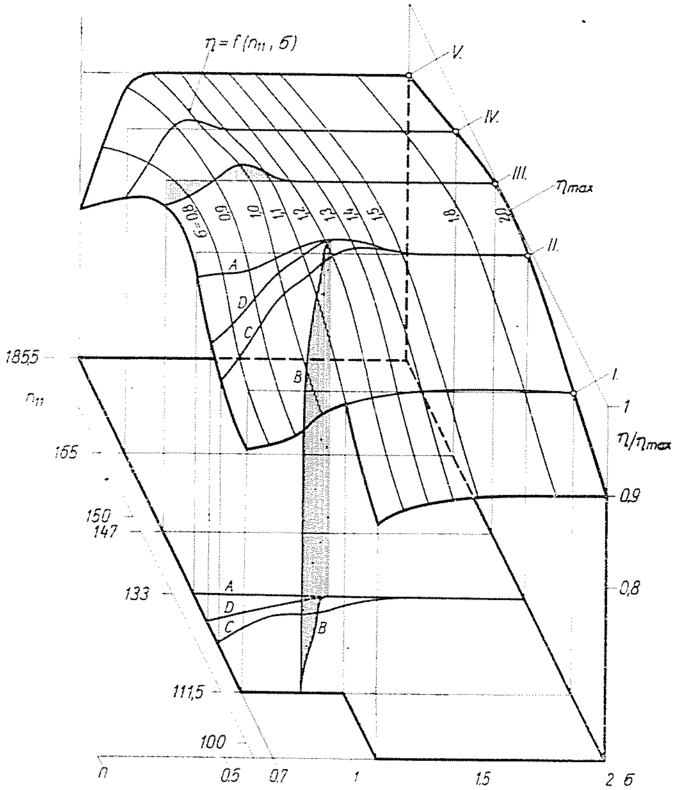

Fig. 5

In Fig. 3, the points meeting conditions A or B fall onto straight lines, whereas condition D indicates parabolae. Condition C means straight lines in Fig. 4. The curves corresponding to the latter lines in Fig. 3 can be plotted by determinating the intersections of the straight lines and $\sigma =$ const curves in Fig. 4, that is, the corresponding n_{11} and σ values, then finding these points in Fig. 3. The respective points can be transferred to Fig. 5 in a similar manner (see operating condition No II).

Applying one of the A, B, C, D methods in the cavitation tests of the turbine, the point indicating the operating condition of the turbine will travel along the corresponding curve in the Figures.

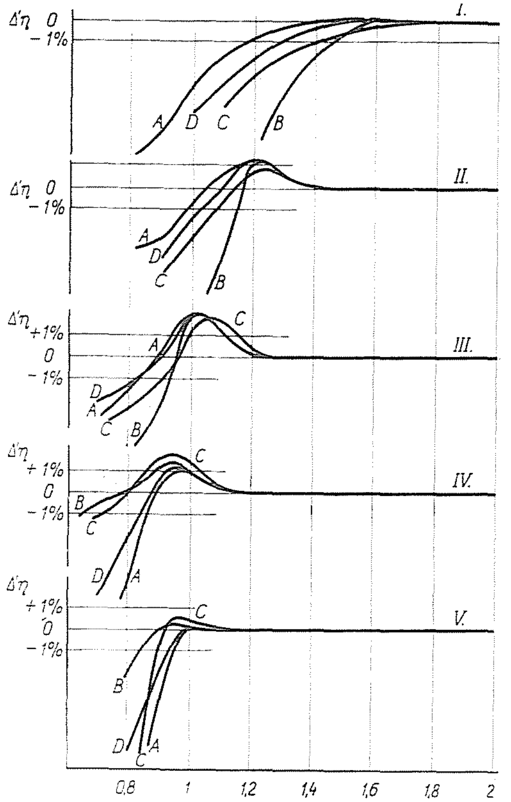

Fig. 6

The Figures permit the plotting of the variation of characteristics in function of σ as it is shown in Figs 6, 7 and 8 where the percentage variation of the individual variables are indicated, for example

$$\Delta' n = \frac{n - n_0}{n_0}$$

Fig. 6 reveals that the various $\Delta'\eta - \sigma$ curves types considerably differ from one another. The sequence of the $\Delta'\eta - \sigma$ characteristic curves in operating conditions I and II is about the reverse of that in operating conditions IV and V. Fig. 5 explains this in an illustrative manner. On the surface $\eta = f(n_{11}, \sigma)$, the A, B, C and D-type characteristic curves are found at the sections obtained for the $n_{11} - \sigma$ curves in plane $[n_{11}, \sigma]$, (see operating condition II). The arrangement of the latter curves in plane $[n_{11}, \sigma]$ is similar in each of the operational conditions as revealed also by Fig. 2. At the ascent of the efficiency peak, however, the $\eta - \sigma$ curves corresponding to the $n_{11} - \sigma$ curves are of an exactly opposite sequence if compared to the curves obtained

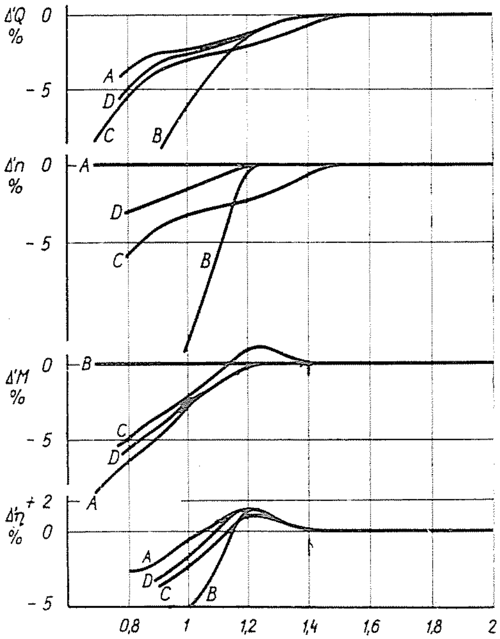

II. operating condition

Fig. 7

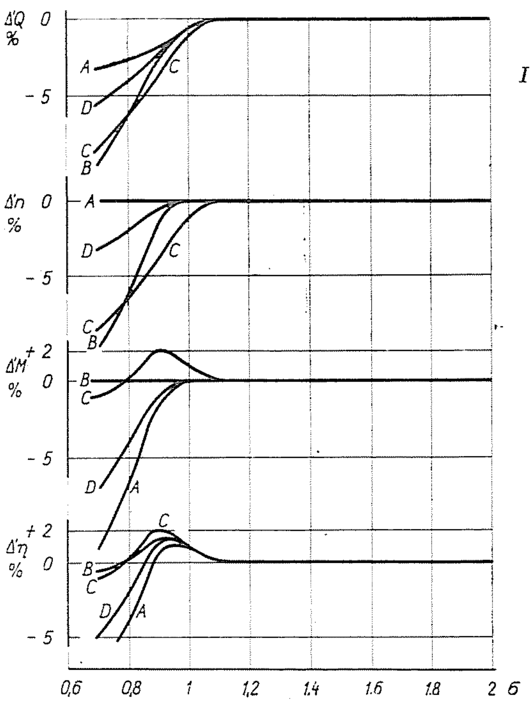

IV. operating condition

Fig. 8

at the other side. Thus, the sequence of the different type $\eta - \sigma$ curves depends on which side of the efficiency peak they might fall to.

Curves $\eta - \sigma$ reveal that a σ decrease leads to a provisional efficiency increase. In order to thoroughly explain this phenomenon, the characteristic curves $Q - \sigma$, $n - \sigma$, $M - \sigma$ were plotted for operating conditions II and IV (Figs 7 and 8). Here the course of curves A, B, and D show that the volumetric flow starts to decrease at σ values higher than do the speed and the torque breakdown value. Thus, the transitory efficiency increase may be attributed, in these cases, to a reduced volumetric flow for an unchanged power output.

Figs 7 and 8 reveal that the steepest "breakdowns" are rendered by the B-type curves. This is why for a number of test series performed in the Ganz-MÁVAG Laboratory the B-type $n - \sigma$ curves were used to determine the "standard σ". Since, according to condition B, $M =$ const, curve $\Delta' n - \sigma$ will be identical to the $\Delta' P - \sigma$ curve as well.

Figs 7 and 8 similarly show that the A and D-type curves are fairly close to each other. Instead of the A-type characteristic curves, therefore, type D may also be used, if tests can be accelerated thereby, and some minor differences may be neglected.

Summary

The course of characteristic cavitation curves depends on the initial cavitation-free operating condition, and on the type of the characteristic curves governed, in course of the tests, by the method of operating condition adjustments.

In case of minor head variations the usual conversion laws may be applied, and, consequently, curve types may be characterized by an equation, each.

The sequence of the different type η—σ characteristic curves depends on which side of the efficiency peak they are. In the tests presented, the temporary efficiency increase at an unchanged power output was due to a slight volumetric flow reduction. Of the P—σ curve types tested, the steepest breakdown was shown by type B defined by $H =$ const, $M =$ const.

If cavitation tests are to be carried out with a model turbine, the most suitable characteristic curve type can be selected by taking both the test objectives and the viewpoints described above into consideration.

References

1. International Test Code for Cavitation Acceptance Tests. Draft of IEC Recommendation, 1965 July.
2. FÁY, Á.: Die Schätzung der Beaufschlagung und des Momentes der Kaplan-Turbine für den Betriebszustand entwickelter Kavitation. Vorträge der II. Konf. für Strömungsmaschinen, Budapest, 24—29 Okt. 1966.
3. OSTERWALDER, J. and LECHER, V.: Influence of head and air content on cavitation. Société Hydrotechnique de France, Symp. de Nice, 16—20 Sept. 1960.
4. WINTERNITZ, F. A. L.: Cavitation in Turbomachines — Water Power, 1957 Oct.
5. SAITO, S.: Effect of the Clearance Cavitation Concerning High Head Kaplan Turbines. Proc. IAHR Symp., Sendai, Japan 1962.
6. HUTTON, S. P.: Über die Voraussage des Verhaltens von Wasserturbinen auf Grund von Modellversuchen. Schweiz. Bauztg. II, 371 (1959).

Dr. Árpád FÁY; Budapest, XI., Sztoczek u. 2—4. Hungary